ELSEVIER

Laminar–turbulent transition in a bayonet tube

Harpal Minhas and G. S. H. Lock
Department of Mechanical Engineering, University of Alberta, Edmonton, AB, Canada

This paper provides the details of a numerical study of the bayonet tube during the laminar–turbulent transition. Attention is focused on the frictional characteristics of the tube. The results constitute a systematic investigation of the effect of the principal parameters on hydraulic resistance represented by an Euler number. Specifically discussed are the effects of fluid properties, tube length, and inner tube width. The data are interpreted in terms of the origin and spread of turbulence, as revealed by the turbulence intensity contours in the k-ϵ model. Comparisons are made with available experimental data.

Keywords: laminar–turbulent transition; bayonet tube; heat exchanger

Introduction

The bayonet tube is a refluent heat exchanger. As shown in Figure 1, it is constructed from two concentric tubes with one end of the inner tube (diameter d) reaching to within a distance H from the sealed end of the outer tube (diameter D). Fluid flowing down inside the inner tube is thus constrained to return along the annular gap formed between the two tubes. The device is particularly useful in situations where the medium to be heated or cooled is either too large to be treated in its entirety or is readily accessible from one side only. The medium is then penetrated by the insertion of bayonet tube, in contrast to more common arrangement of tubes crossing back and forth.

Bayonet tube use in geophysical and industrial applications has been discussed extensively (Lock 1992; Lock and Wu 1993; Minhas et al. 1995). Biomedical applications include cryosurgery (Cooper 1967). The technique utilizes bayonet tubes as a cryoprobe for producing very low localized temperatures. This phenomenon is used for selective destruction of damaged tissues. The method has been found to be safe and effective.

The device has been studied experimentally by Idel'Chik and Ginzburg (1968). They discovered a strong influence of clearance ratio. During a numerical study in 1988, Yang and Hsieh detected a vortex in the end clearance zone. The end vortex was explored further by Minhas (1993) and Minhas et al. (1995). Lock and Wu (1993) presented experimental data on the effects of mass flow rate and tube geometry on the thermal performance of the tube.

This paper extends the earlier work of Minhas et al. (1995), which was restricted to fluid flow characteristics under laminar conditions. Particular attention is focused on the laminar–turbulent transition. A numerical analysis is used to explore the origin and spread of turbulence. The study of pressure drop has been conducted over a wide range of important variables: fluid properties, Reynolds number, width–diameter ratio and length–diameter ratio. The area ratio, F_i/F_a, where F_i, F_a are the inner and annular flow areas, respectively, was fixed at 0.474, and the clearance ratio H/D at 1.0; these values correspond to an "optimal" in the hydraulic design (Minhas et al.). Comparison are made with earlier experimental data.

Numerical analysis

Governing equations and boundary conditions

Flow in a bayonet tube is governed by the continuity and momentum equations. Neglecting buoyancy, the governing equations for steady, turbulent flow of a Newtonian fluid may be written as follows;

Continuity:

$$\nabla \cdot \rho U = 0 \tag{1}$$

Momentum:

$$\nabla \cdot (\rho U \times U) = \nabla \cdot (\sigma - \rho \overline{u \times u}). \tag{2}$$

where

$$\sigma = -p\delta + \mu\left(\nabla U + (\nabla U)^T\right) \tag{3}$$

The above equations were cast in cylindrical coordinates assuming axisymmetry.

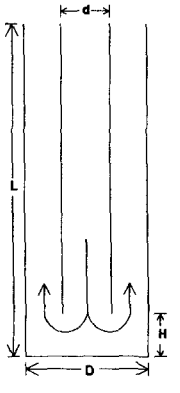

Figure 1 Dimensions of the bayonet tube

Address reprint requests to H. Minhas, Deparment of Mechanical Engineering, University of Alberta, 4-9 Mechanical Engineering Bldg., Edmonton, AB T6G 2G8, Canada.

Received 26 May 1995, accepted 28 August 1995

Int. J. Heat and Fluid Flow 17: 102–107, 1996

655 Avenue of the Americas, New York, NY 10010

0142-727X/96/$15.00
SSDI 0142-727X(95)00078-X

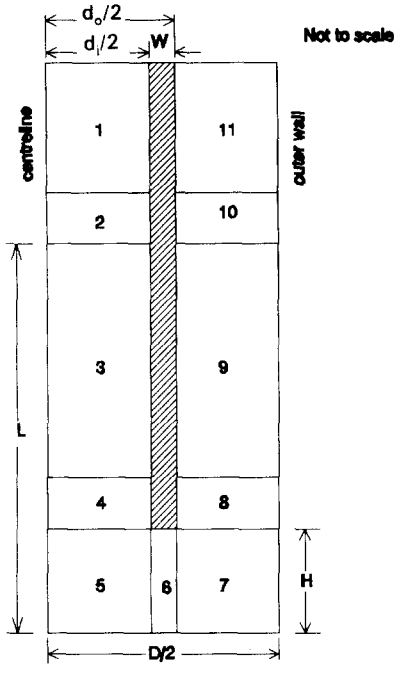

Figure 2 Computational domain

Boundary conditions were handled as follows. Long, extension tubes ($L/D \approx 200$) attached to the upper end of the bayonet tube were used to create realistic conditions at inlet and outlet (see Figure 2). A hydrodynamically fully developed condition was thus obtained at the entrance to the inner tube, while a Neumann condition (zero axial gradients) was established at the extension tube outlet. The velocity at all walls was taken to be zero. Symmetry and periodicity were assumed at the tube center and periodicity plane ($\theta = 0, 2\pi$), respectively.

Definitions

The results given below are expressed in terms of the following parameters, divided into three categories:

Geometry.

(1) *Width–diameter ratio*: W/D, where W and D are the inner tube width and outer tube diameter, respectively;
(2) *Length–diameter ratio*: L/D, where L and D are the length and diameter, respectively, of the outer tube;
(3) *Area ratio*: F_i/F_a, where F_i and F_a are the inner tube and annulus areas, respectively. *
(4) *Clearance ratio*: H/D, where H is the end clearance of the inner tube. †

Flow rate. *Reynolds number*: Following Lock and Wu (1991), the Reynolds number is defined by the following:

$$\mathrm{Re} = \frac{4\dot{m}D}{\rho\pi\nu(D + d_0)d_i} \tag{4}$$

where d_0, d_i are the outside and inside diameters of the inner tube, respectively: $W = (d_0 - d_i)/2$. This was chosen to accommodate the appropriate form of the Reynolds number for limiting cases of $d_i \ll D$ and $D \approx d_i$.

Pressure drop. *Euler number*: Again, following Lock and Wu (1991), the Euler number Eu was taken as:

$$\mathrm{Eu} = \frac{2\Delta P}{\rho(U^c)^2} \tag{5}$$

where

$$\Delta P = \Delta P_t + \rho U_i^2\left[1 - \frac{3}{4}\left(\frac{E_i}{F_a}\right)^2\right] \tag{6}$$

and the characteristic velocity scale U^c is given by

$$U^c = \frac{4\dot{m}D^2}{\rho\pi\left(D^2 - d_o^2\right)d_i^2}. \tag{7}$$

Properties were evaluated at a temperature of 343 K.

Algorithm and program validation

The numerical analysis was performed using version 3.2.1 of Flow3d package of Harwell Laboratory in the UK. The SIMPLE-C algorithm (Van doormal and Raithby 1984) was incorporated.

* This was held constant at the "optimal" value (0.474) found in previous laminar work (Minhas et al. 1995).
† This was also held constant at the "optimal" value (1).

Notation

c	coefficient
d	inner tube diameter
D	outer tube diameter
F	flow area
H	end clearance
i	turbulence intensity
k	turbulent kinetic energy
L	overall length of bayonet tube
m	mass
P,p	pressure
Re	Reynolds number
u	turbulent velocity
U	velocity
W	thickness of inner tube

Greek

ρ	mass density
μ	fluid dynamic viscosity
ν	momentum diffusivity
ϵ	rate of dissipation of turbulent kinetic energy
θ	circumferential distance

Subscripts

a	annulus
d,i	inner tube
o	outer

Superscripts

$\cdot$	per unit time
c	characteristic
T	transpose

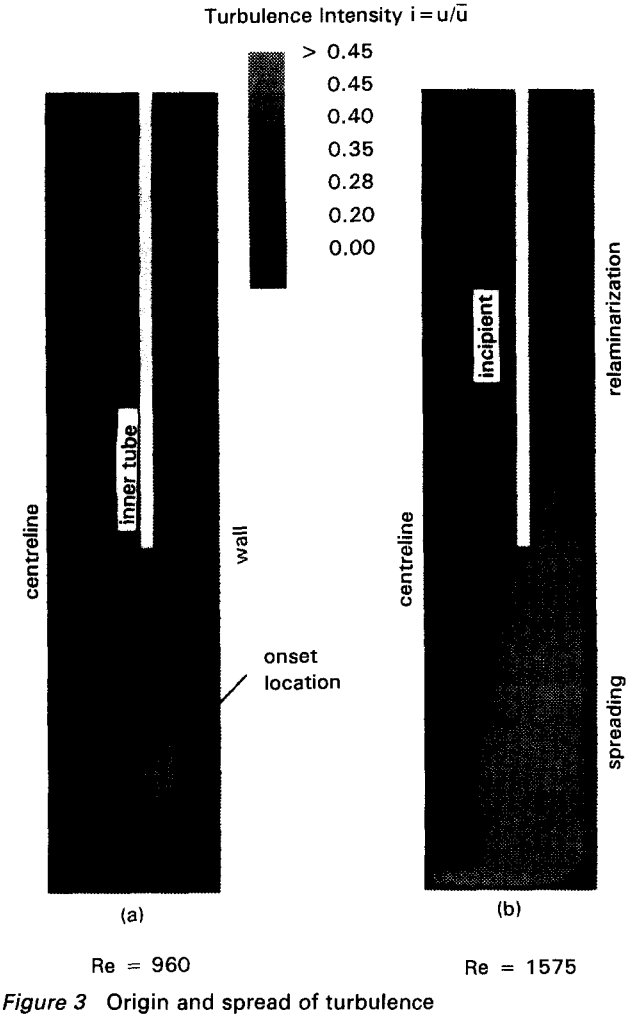

Figure 3 Origin and spread of turbulence

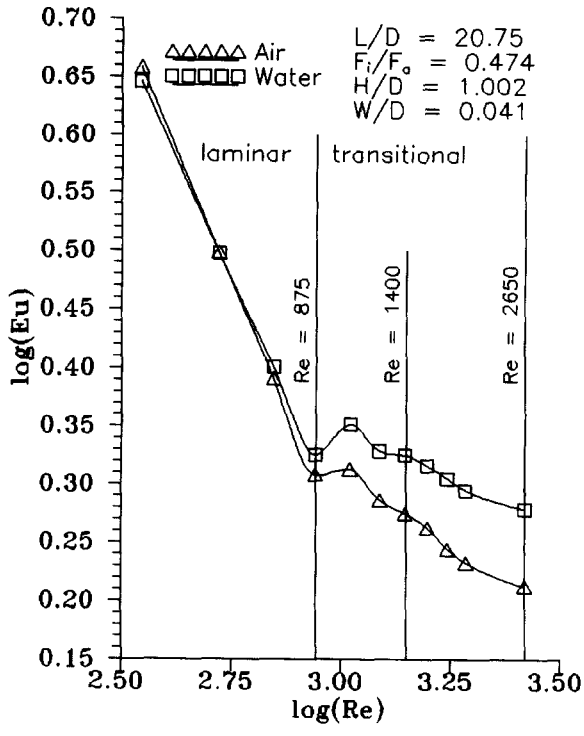

Figure 4 Effect of fluid properties on Euler number

Stone and preconditioned conjugate gradients methods were used to solve the linearized velocity and pressure-correction equations, respectively. Turbulence was modeled using a low-Reynolds number k-ϵ model (Jones and Launder 1972). This is well established in recirculating flows and does not require a laminar–turbulent switch. It has been successfully applied to relaminarizing flows (Launder and Sharma 1974).

The computational domain was divided into 11 blocks (see Figure 2). A 20×20 grid was used for blocks 1, 2, 3, 4, 8, 9, 10, and 11, respectively. It was anticipated that a finer grid would be needed to accommodate a more complex field in the end clearance space. A 40×40 grid for blocks 5 and 7, respectively, and a 40×4 grid for block 6 were, therefore, used. A convergence factor of 0.65 was used. The convergence criterion required agreement of successive averaged values of the dependent variables to be within 1%.

The program was first run at "standard" parametric values: $\mathrm{Re} = 875$, $L/D = 20$, $F_i/F_a = 0.474$ and $H/D = 1$ represent practical operational values for a bayonet tube (Lock and Wu 1991). As discussed later, the above Reynolds number represents the onset of the laminar–turbulent transition. An accuracy test with the grid size halved indicated an Euler number change of less than 3%, while the time taken to run the program was then increased by more than 10 times. The program run in three dimensions indicated an Euler number change of less than 3%. Spot checks with different initial fields produced identical results thus suggesting unique solutions.

Discussion of results

Origin and evolution of turbulence

Frictional behavior was studied assuming the tube surfaces to be smooth. Results were obtained for the Reynolds number range $350 < \mathrm{Re} < 2650$. For the geometry chosen, the inner tube and annulus Reynolds numbers are given by $\mathrm{Re}_d = 1.62\mathrm{Re}$ and $\mathrm{Re}_a = 0.56\mathrm{Re}$, respectively. Within the inner tube, the onset of turbulence was expected to occur near $\mathrm{Re} \approx 1480$, corresponding to $\mathrm{Re}_d = 2400$. As Figure 3 demonstrates, the contours of turbulence intensity $i = (2k/3)^{0.5}/\bar{u}$, where $\bar{u}$ is the mean inlet velocity at $\mathrm{Re} = 1400$, revealed that turbulence begins earlier. Numerical data indicates that onset occurs at $\mathrm{Re} \approx 875$. This created a marked change in the Eu–Re curve, as will be seen later. Figure 3a suggests that turbulence originates in the high-shear field in the clearance zone where random disturbances are not easily damped by an adjacent wall. Turbulence fluctuations grow rapidly beyond $\mathrm{Re} = 875$, as Figure 3a shows. The narrow space in the annulus tends to damp the turbulent fluctuations, thereby producing a gradual return to laminar conditions. At $\mathrm{Re} = 1400$, the flow in the inner tube became turbulent. As shown in Figure 3b, at $\mathrm{Re} = 1575$, the turbulent effects are significant in the inner tube. As expected, the relaminization front moved downstream with an increase in Reynolds number. The flow became fully turbulent throughout the bayonet tube at $\mathrm{Re} = 2650$; that is, with $i > 0.8\%$ (0.08) at the exit.

Effect of fluid properties

In a previous study of air (Minhas et al. 1995) under laminar conditions, it was anticipated that a change in fluid properties would not affect the friction coefficient. This cannot be assumed under turbulent or transitional conditions. A comparison of gaseous and liquid behavior was, therefore, undertaken using air and water. The results are plotted in Figure 4, as an Eu–Re plot.

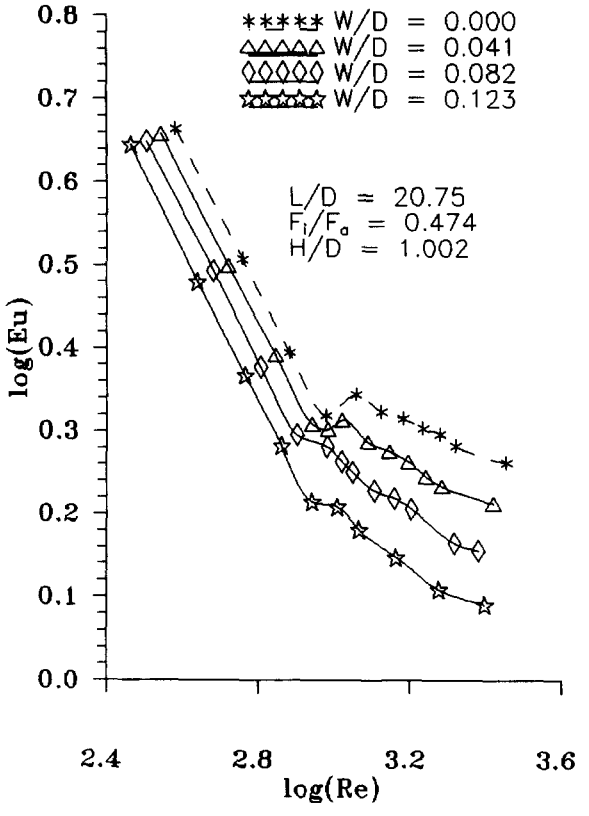

Figure 5 Effect of inner tube thickness on Euler number

As expected, the curves are virtually coincident in the laminar regime. At Re = 875, corresponding to the onset of turbulence in the clearance space, a sudden change in slope is noted. After this, flow resistance is not only higher than under laminar conditions but is seen to be a more complex function of flow rate. The critical Reynolds number for the inner tube is reached at about Re = 1480; i.e., $Re_d = 2400$. This is marked by entry to a monotonically decreasing portion of the Eu–Re curve extending up to the limit of transition within this particular tube. The curves follow a similar trend in the transitional regime with the maximum difference being 16% (of air). The turbulence intensity plots for these fluids were compared at the same mass flow rate. Turbulence intensities for water were greater than for air. This suggests that the weaker damping is less viscous fluids is the cause of the reduction in Euler number.

Effect of inner tube width

Figure 5 shows the effect of inner tube wall thickness on Euler number, assuming D and F_i/F_a are fixed and the no-slip boundary condition is maintained, even when $W = 0$. It is evident that onset of turbulence in both the clearance zone and the inner tube are essentially independent of width–diameter ratio, although the precise shape of the curve does vary in the transitional range. At first thought, the decrease in Eu with W/D appears to be counterintuitive. However, from Equation 7, for same area ratio and outer tube diameter, an incremental change in the characteristic velocity with inner tube diameter, may be written as follows:

$$\frac{(U^c)_{d_i+\Delta d_i}}{(U^c)_{d_i}} \approx \frac{1}{\left(1-\dfrac{\Delta d_i}{d_i}\right)^4} \tag{8}$$

where

$$\Delta d_i = \left\{ d_i + c(\Delta W + d_o) + \left(\left[d_i + c(\Delta W + d_o) \right]^2 - (c+1)\left\{ d_i^2 - c\left[D_2 - d_0^2 - (\Delta W)^2 + 2 d_o \Delta W \right] \right\} \right)^{1/2} \right\} \times (c+1)^{-1} \tag{9}$$

where $\Delta W = 2\Delta w$, Δw being the change in inner tube width, and c is the area ratio F_i/F_a. Thus, as Δd_i increases with increasing W/D, U^c also increases, lowering Eu. The increase in U^c resulting from the physical blockage of a thicker inner tube evidently causes the lowering of the Eu–Re curve seen in Figure 5.

Effect of length–diameter ratio

In the earlier study (Minhas et al. 1995), it was found that $F_i/F_a = 0.474$ and $H/D = 1.0$ correspond to an optimal hydraulic design; i.e., a local minimum in Euler number. They were, therefore, held constant at these values during the present study, while the length–diameter ratio was varied in the representative, practical range $10 < L/D < 40$. This effect is shown in Figure 6, where the Euler number is plotted as a function of Re and L/D. The numerical results for the "standard" geometry $L/D = 20.75$ may be compared with the available experimental data (Lock and Wu 1991). Agreement is within the experimental error of $\pm 10\%$. The onset and development of turbulence are evidently independent of L/D. As expected, Euler number decreases monotonically with increasing L/D.

Empirical correlation

The results given above systematically uncover the effect of flow rate, fluid properties, and tube length on hydraulic behavior during the laminar–turbulent transition. However, in the form presented, they are limited in their direct application to a wide range of industrial and geotechnical problems. To circumvent this

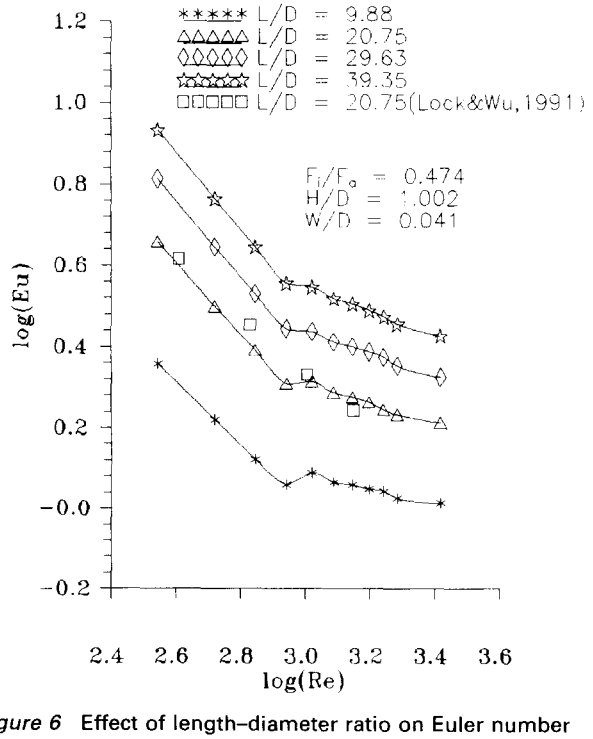

Figure 6 Effect of length–diameter ratio on Euler number

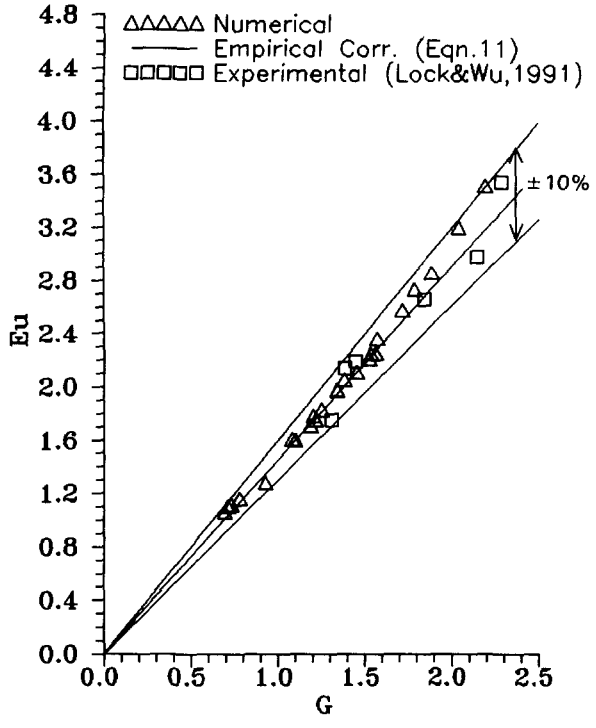

Figure 7 Empirical correlation

restriction, the entire set of numerical data were used to develop an empirical correlation with Euler number as the dependent variable. The results are shown in Figure 7.

To construct a suitable empirical correlation form it was decided that the effect of length–diameter ratio could be accurately represented by a power law. A similar assumption was also made for the effect of Reynolds number, but Figure 4 reveals this to be only a rough approximation under transitional conditions. However, for design purposes, a more accurate curve fit does not seem warranted. The effect of width–diameter ratio was introduced through a simple complementary power-law form. The general relationship was, thus, sought in the product form.

$$\mathrm{Eu} = \frac{c_f(\nu)\left[\frac{L}{D}\right]^{\alpha}\left[1-\frac{W}{D}\right]^{\beta}}{\mathrm{Re}^{\gamma}} \tag{10}$$

where α, β, and γ are exponents, and the coefficient $c_f(\nu)$ is a function of fluid properties. This empirical correlation yielded the following:

$$\mathrm{Eu} = C_f G \tag{11}$$

where

$$G = \frac{\left[\frac{L}{D}\right]^{0.72}\left[1-\frac{W}{D}\right]^{2.82}}{\mathrm{Re}^{0.25}} \tag{12}$$

and $c_f = 1.45$ for air and 1.6385 for water. The exponent of L/D is close to the value of 0.75 found under laminar condition (Minhas et al. 1995).

Figure 7 shows Equation 11 superimposed on the experimental data for air (Lock and Wu 1991) and representative numerical data from the present study. The data fall within a band of $\pm 10\%$. This uncertainty is greater than the intrinsic numerical accuracy of $\pm 3\%$, mainly because of the approximations inherent in the assumed power-law forms, especially with respect to Re. It is, however, acceptable for most industrial and geoetechnical applications of the bayonet tube when F_i/F_a and H/D are fixed near the "optimal" values of 0.474 and 1.0, respectively.

Conclusions

This paper presents numerical data for steady fluid flow in a bayonet tube during the laminar–turbulent transition. The results apply to a cylindrical tube with the area and clearance ratios fixed at their "optimal" values. Hydraulic resistance, as indicated by the Euler number, was investigated in terms of the Reynolds number, width–diameter ratio, and length–diameter ratio. Parametric effects were examined in relation to turbulence intensity plots. Good agreement with previous experimental data was demonstrated.

The onset of turbulence was marked by a sudden change in slope of the Eu–Re curve near Re = 875. The velocity field data revealed that transition begins in the clearance zone where the damping influence of adjacent walls is most limited. Thereafter, an increase in Reynolds number causes the turbulent field to spread until turbulence is generated inside the inner tube. Beyond that particular Reynolds number, turbulence spreads downstream in the annular region where a damping tendency causes a return to laminar conditions. However, a sufficiently high Reynolds number (2650) leads to a completely developed turbulent field throughout the device.

The effect of fluid properties following transition was significant. This was attributed to a lower damping in less viscous fluids.

The width–diameter ratio influence on Euler number was also significant. The decrease in Euler number with increasing W/D was attributed principally to an increased velocity.

The Euler number decreased monotonically with increasing L/D, as expected, the influence being nearly the same as under laminar conditions.

The effects of individual parameters were combined in a simple empirical correlation. The correlation may be useful for designers concerned with hydraulic behavior during the laminar–turbulent transition.

Acknowledgments

This work was made possible through the support of Natural Sciences and Engineering Research Council of Canada, to whom we are indebted. We also wish to thank Mark Ackerman for assistance in the use of computational facilities in the Mechanical Engineering Department.

References

Cooper, I. S. 1967. Cryogenic surgery. In *Engineering in the Practice of Medicine*, B. L. Segal and D. G. Kilpatrick (eds.), Williams & Wilkins, Baltimore, MD, 122–141

Idel'chik, I. E. and Ginzburg, Y. L. 1968. The hydraulic resistance of 180° annular bends. *Teploenergetika*, **4**, 109–114

Jones, W. P. and Launder, B. E. 1972. The prediction of laminarization with a two-equation model of turbulence. *Int. J. Heat Mass Transfer*, **15**, 301–314

Launder, B. E. and Sharma, B. T. 1974. Application of the energy dissipation model of turbulence to the calculation of flow near a spinning disc. *Lett. Heat and Mass Transfer*, **15**, 1787

Lock, G. S. H. and Wu, M. 1991. Laminar frictional behavior of a bayonet tube. *Proc. 3rd Int. Symp. on Cold Regions Heat Transfer*, Fairbanks, AK, 429–440

Lock, G. S. H. 1992. *The Tubular Thermosyphon.* Oxford University Press, Oxford, UK

Lock, G. S. H. and Wu, M. 1993. Heat transfer characteristics of bayonet tube using air under laminar conditions. *Int. J. Heat Mass Transfer*, **36**, 287–291

Minhas, H. S. 1993. The bayonet tube: A numerical analysis of laminar frictional characteristics. Master's thesis, University of Alberta, Edmonton, AB, Canada

Minhas, H., Lock, G. S. H. and Wu, M. 1995. Flow characteristics of an air-filled bayonet tube under laminar conditions. *Int. J. Heat Fluid Flow*, **16**, 186–193

Van doormal and Raithby, G. D. 1984. Enhancement of the SIMPLE method for predicting incompressible fluid flows. *Num. Heat Transfer*, **7**, 147–163

Yang, S. L. and Hsieh, C. K. 1988. Fluid flow and heat transfer in a single pass, return flow, bayonet heat exchanger. *Proc. ASME, AICHE, Nat. Heat Transfer Conference*, Houston, TX, **3**, 355–364.